Article

Journal of
Biomedical Nanotechnology
Vol. 18, 1–10, 2022
www.aspbs.com/jbn

In Vitro Evaluation of Ultrasound Effectiveness in Controlling Doxorubicin Release from Albumin-Conjugated Liposomes

Waad H. Abuwatfa[1, 2], Vinod Paul[1, 2], Nour M. AlSawaftah[1, 2], Afifa Farooq[1], Nahid S. Awad[1], and Ghaleb A. Husseini[1, 2, *]

[1] *Department of Chemical Engineering, College of Engineering, American University of Sharjah, Sharjah, 26666, UAE*
[2] *Materials Science and Engineering Program, College of Arts and Sciences, American University of Sharjah, Sharjah, 26666, UAE*

Functionalized liposomes are among the most promising antineoplastic agents delivery vehicles. Contemporaneous to their accretion at the tumor site, they need to be potentiated to release their cargo using a suitable triggering modality. In this work, targeted DOX-loaded stealth liposomes were synthesized and functionalized with Human Serum Albumin (HSA) to target the overexpressed HSA receptors (HSA-Rs). The effects of low-frequency ultrasound (LFUS) in inducing DOX release from the synthesized liposomes were investigated *in vitro*. DOX release increased with the increasing power density of the ultrasound. HSA conjugation to the liposomes increased their sensitivity to LFUS. Furthermore, HSA conjugation also enhanced the liposome's cytotoxic activity and uptake by the cancer cells overexpressing HSA-Rs. This cytotoxic activity and cellular uptake were further enhanced by triggering drug release from those targeted liposomes using LFUS. Combining HSA-targeted liposomes with LFUS is a promising approach in drug delivery.

KEYWORDS: *Human Serum Albumin (HSA), Liposomes, Low-Frequency Ultrasound (LFUS), Controlled Release, Cell Viability.*

INTRODUCTION

Genetic alterations, often present as gain-of-function (GOF) or loss-of-function (LOF) mutations, can cause an increase in cell proliferation potentials, while simultaneously turning off growth regulatory mechanisms. Cancer is the uncontrolled division of diseased cells due to DNA mutations. Enduring research efforts towards exploring potential technological advances in cancer therapy modalities have intensified in recent years. Standard treatments like surgery and/or radiation, often accompanied by a chemotherapy regimen(s) to complete the treatment cycle, have been the traditional curative interventions [1]. Due to the detriment to the patient's quality of life and the potential lethality of some of the side effects associated with conventional treatments, the potential of utilizing receptor-ligand interactions between highly expressed tumoral cell-surface receptors and drug carriers modified with complementary ligands to these specific markers has been widely investigated [2]. Cancerous tumors require an excess supply of nutrients, oxygen and other conditions and thus tend to overexpress certain biological markers on their surfaces to aid in their tumorigenesis and survival pathways. Several types of breast tumorigenesis have been linked to the overexpression of heterogeneous nuclear ribonucleoproteins (HSA-Rs), specific receptors of the human serum albumin (HSA) protein [3–5]. While tumoral vascular structures are characterized by their irregular defective nature and the lack of proper lymphatic drainage and fluid transport dynamics, these features inspired the development of nanocarrier-based drug delivery platforms [6].

Nanocarriers like liposomes, micelles and dendrimers can extravasate into the tumor's interstitium and accumulate in the disorganized neovasculature of these malignant tissues, delivering the drug to the desired anatomical locations. This phenomenon is known as the enhanced permeability and retention (EPR) effect [7]. Liposomes have proven to be stable and effective nanocarriers that the

*Author to whom correspondence should be addressed.
Email: ghusseini@aus.edu
Received: 22 July 2022
Accepted: 24 September 2022

FDA approved after successful clinical trials in 1995 [8]. Liposomes are prepared from different phospholipids formulations with high compatibility and excellent ability to encapsulate hydrophilic and hydrophobic antineoplastic drugs. The prolonged circulation of the liposomes can be achieved by decorating their surfaces with stealth imparting polymers such as polyethylene glycol (PEG). Furthermore, liposomes can be engineered with a wide range of targeting ligands that recognizes and bind to specific tumor neoantigens overexpressed on the cancer cells [8]. Some examples include carbohydrates, proteins, and antibodies, in addition to small molecules (e.g., estrone and folic acid). Moreover, different internal and external stimuli can be employed to trigger drug release from liposomes and the other nanocarriers in a controlled manner. These triggers include pH, redox potential, temperature, electromagnetic waves, enzymes, ultrasound, and light. Ultrasound (US) is considered one of the most important, versatile and useful drug release modalities due to its non-invasiveness, safety, and relatively low costs. Although it is best known in the medical field for its imaging applications [9], US has proven to be a powerful theranostic tool, especially in the field of cancer treatment and triggering drug release from liposomes [9–12].

There are two mechanisms by which US can induce biological effects, thermal and mechanical. The mechanical effects of US manifest as cavitation events. Cavitation occurs when the energy produced from ultrasound waves drops the liquid's static pressure below its vapor pressure, causing small vapor-filled cavities to form, grow, and oscillate in the liquid medium. Depending on the behavior of the oscillating bubble, cavitation can be classified as stable or inertial (transient or collapse) cavitation. In stable cavitation, the bubbles oscillate around an equilibrium radius value in each acoustic cycle. In collapsed cavitation, the formed bubbles grow, oscillate, and rapidly expand to up to three-fold their resonance size and eventually collapse [13]. Subsequently, microstreams and shock waves are also generated, which disturb nearby cells and tissues. It is believed that this is the main mechanism by which US-mediated release from nanocarriers is induced [13, 14]. Apfel and Holland [15] proposed the calculation of a Mechanical Index (MI), which serves as an indicator of the US's ability to induce cavitation-associated bio-effects. It is calculated by dividing the peak negative pressure of the US beam by the square root of its center frequency. A MI greater than 0.3–0.4 is considered sufficient to initiate transient cavitation events in the insonated media. According to the FDA, a MI of 1.9 is the allowed threshold for the safe, non-damaging application of US, beyond which micromechanical damage can occur.

This study aims to prepare DOX-loaded stealth liposomes functionalized with HSA and investigate their targeting efficiency using a breast cancer cell line overexpressing HSA-Rs. Furthermore, the ability of low-frequency ultrasound (LFUS) to trigger drug release from the stealth liposomes (DOX-Lip) and albumin-bound liposomes (HSA-DOX-Lip) will be evaluated.

EXPERIMENTAL DETAILS

Materials

Doxorubicin hydrochloride was purchased from Euro Asia (Mumbai, India). 1,2-distearoyl-sn-glycero-3-phosphoethanolamine-N-[amino(polyethylene glycol)-2000] (DSPE-PEG(200)-NH_2) and 1,2-dipalmitoyl-sn-glycero-3-phosphocholine (DPPC) were obtained from Avanti Polar Lipids Inc. (Alabama, USA, supplied by Labco LLC. Dubai, UAE). The QuantiPro™ bicinchoninic acid (BCA) kit was bought from Sigma Aldrich Chemie GmbH (Munich, Germany). Cholesterol (≥99%), HEPES sodium salt, chloroform, Sephadex® G-25, cyanuric chloride (2,4,6-Trichloro-1,3,5-triazine), Human Serum Albumin (HSA, ≥98%) powder, Ammonium sulfate salt ($(NH_4)_2SO_4$), Triton X-100, Dulbecco's Modified Eagle Medium (DMEM) and RPMI-1640 medium were purchased from Sigma–Aldrich Chemie GmbH (supplied by Labco LLC. Dubai, UAE).

Preparation of Liposomes

As described by Zhang, liposomes were prepared using a modified thin-film hydration method [16]. In brief, DPPC, DSPE-PEG(2000)-NH_2, and cholesterol were added to a round bottom flask at a molar ratio of 65:5:30, respectively and were dissolved in chloroform (4 mL). To evaporate the chloroform and form a thin lipid film, the solution was heated to 50 °C using a rotary evaporator in vacuum for 15 min. Next, the formed lipid film was hydrated with $(NH_4)_2SO_4$ solution (0.11 M) at a pH of 5.5 at 60 °C for 50 min. Next, the liposomal suspension was sonicated using a 35-kHz ultrasonic bath for 2 min (Elma D-78224, Illinois, USA) to obtain unilamellar liposomes. The liposomes were extruded at 60 °C using an Avanti® mini-extruder assembly (Avanti Polar Lipids, Inc., Alabama, USA) through 0.2-μm polycarbonate filters. DOX encapsulation was carried out using the remote $(NH_4)_2SO_4$ transmembrane gradient method [17]. The liposomes were passed through a HEPES column at pH 7.4 to create the pH gradient. DOX (16 mg per 1 mL HEPES buffer) was added to the liposomal solution at a ratio of 1:6 (w/w), respectively. The solution was left to stir for 45 min at 60 °C. The loaded liposomes were purified through size exclusion chromatography in a Sephadex G-25 gel column equilibrated with a phosphate-buffered saline solution (PBS) at pH 7.4. The collected liposomes were used as the control, referred to as DOX-Lip.

Preparation of HSA-DOX-Liposomes

To initiate the HSA conjugation reaction, the DOX-loaded liposomes were alkalized by passing them through another Sephadex G-25 gel column equilibrated with borate buffer

(pH 8.5). A double-displacement conjugation reaction using cyanuric chloride (CC) was used (Fig. 1). Liposomes were incubated with 28 μL of CC solution (10 mg of CC powder/1 mL pure acetone + 0.5 mL distilled water) for 3 hours in an ice bath at 0 °C. Then, 75 μL of the HSA solution (10 mg HSA powder/1 mL borate buffer) was added and the liposomes were left to stir overnight. The conjugated liposomes (HSA-DOX-Lip) were then filtered using size exclusion chromatography and stored at 4 °C until further use.

Size and Polydispersity Measurements

Dynamic light scattering (DLS) was employed to determine the hydrodynamic radius, polydispersity, and size distribution of the prepared liposomes at room temperature using the DynaPro® NanoStar™ (Wyatt Technology Corp., CA, USA) DLS machine. The samples were prepared by diluting 15 μL of the liposomes in 1 mL of PBS buffer.

Cell Lines and Culture Conditions

HSA-positive (HSA+) MCF-7 cell line and HSA-negative (HSA-) HeLa cell line were purchased from the European Collection of Authenticated Cell Cultures (ECACC general cell collection, Salisbury, UK). The cells were cultured in Roswell Park Memorial Institute (RPMI-1640) medium and Dulbecco's Modified Eagle Medium (DMEM), supplemented with 10% Fetal Bovine Serum (FBS) and 1% Penicillin/ streptomycin. Cells were incubated in a 5% CO_2 incubator at 37 °C for proliferation.

Quantification of Total Phospholipids Content

The quantification of the phospholipids' content was carried out using the Stewart assay. Briefly, 50 μL of the liposomes was dried in a rotary evaporator under vacuum at 45 °C for 15 min. One mL of chloroform was then added to the flask, followed by sonication for 10 min in a 35-kHz sonicating bath. Two mL of ammonium ferrothiocyanate (FTC) were added to the liposomal-chloroform mixture and centrifuged for 10 min at 1000 rpm. The separated bottom layer containing the formed phospholipid-FTC complex was then collected and transferred to a quartz cuvette. The optical density of each sample was measured at 485 nm using an Evolution™ 60S Ultraviolet-visible (UV-VIS) spectrophotometer (Thermo Fisher Scientific, Massachusetts, USA). Three replicates for each sample were used.

Determination of the Encapsulation Efficiency

The amount of loaded DOX present inside the liposomes (encapsulation efficiency) was determined following the removal of free DOX using gel filtration chromatography (Sephadex G-25). Evolution™ 60S Ultraviolet-visible (UV-VIS) spectrophotometer (Thermo Fisher Scientific, Massachusetts, USA) at $A_{max} = 482$ nm was used to measure the optical density of the diluted liposomes (60x) after the addition of Triton X-100 (1% v/v). A calibration curve, prepared using the absorbance values of different known concentrations of DOX dissolved in HEPES buffer (pH = 7), was used to calculate the final concentration of the entrapped DOX.

Quantification of Protein Content

The albumin conjugation to the liposomes was determined using the bicinchoninic acid (BCA) assay. The BCA reagent was prepared by mixing the QuantiPro QA buffer, QuantiPro QB buffer and $CuSO_4$ solution in the fixed ratio of 25:25:1, respectively. One ml of the prepared reagent was added to an Eppendorf tube together with 600 μl of the PBS buffer and 400 μl of the liposomes followed by an hour of incubation at 60 °C. The optical density of the incubated samples was then measured at 562 nm using the Evolution™ 60S Ultraviolet-visible (UV-VIS) spectrophotometer (Thermo Fisher Scientific, Waltham, MA, USA). Three replicates for each sample were used.

LFUS-Triggered DOX Release

A Low-frequency ultrasonic probe (model VCX750, Sonics & Materials Inc., Newtown, CT) was used to trigger DOX release from liposomes at a frequency of 20 kHz. DOX release was monitored through changes in fluorescence using a QuantaMaster QM 30 Phosphorescence Spectrofluorometer (Photon Technology International, Edison, NJ, USA). DOX has maximum excitation and emission wavelengths of 470 nm and 560 nm, respectively [18]. The initial fluorescence (I_0) is measured for 60 sec to establish a baseline (a fluorescence level without ultrasound). The sample is then sonicated in a pulsed manner (20 sec on, 10 sec off) until a plateau is reached (total

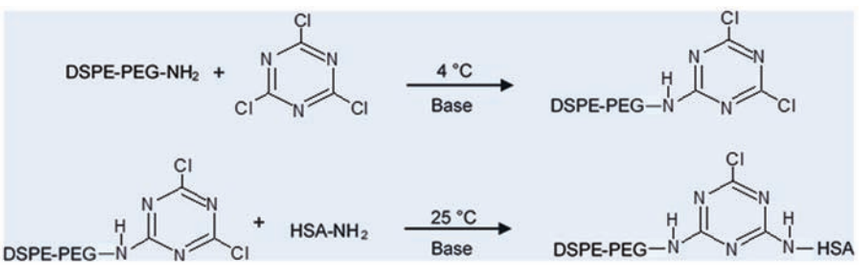

Figure 1. **HSA conjugation to the surface of the liposomes using cyanuric chloride.**

sonication time of 4 min). Triton X-100 is then added to the sample to lyse the liposomes and achieve 100% DOX release. The release is performed at three different power densities, i.e., 6.2 mW/cm^2, 9 mW/cm^2 and 10 mW/cm^2. The cumulative fraction release (CFR) of DOX is calculated using the following equation:

$$\mathrm{CFR} = \frac{I(t) - I_0}{I_{\mathrm{Tx}} - I_0} \times 100\% \quad (1)$$

Where $I(t)$, is the fluorescence intensity value at any time (t), I_0, is the baseline intensity, and I_{TX}, is the intensity after the addition of Triton X-100.

Cell Viability Assay

A modified MTT assay protocol [19] was adopted. MCF-7 (HSA+) cells were cultured in RPMI-1640 and HeLa (HSA-) cells were cultured in DMEM. Cells were seeded in 96-well plates at a density of 1×10^4 cells per well and incubated for 24 hours. The cells were then treated with free DOX (2.9 mg DOX/5 mL DMSO), DOX-Lip or HSA-DOX-Lip with a final DOX concentration of 8 μM. The plates were then incubated for 5 hours after which the sonicated plates were placed in a 35-kHz LFUS sonicating bath for 1 min. The plates were then incubated for 48 hours before carrying out the MTT assay. The incubation time was determined according to the doubling time of the cell lines, based on cell confluency and morphology analyses. Following the post-treatment incubation, fresh media mixed with 10% (v/v) MTT solution was added to the cells, followed by 4 hours of incubation. The media was then discarded and 100 μL of DMSO per well was added to ensure the complete dissolution of the purple formazan crystals. The optical density (OD) at 570 nm was measured using the ELISA M965+microplate spectrophotometer (Metertech, India). Cell viability percentages were calculated as the ratio of the OD values to the mean OD of the control (untreated cells) multiplied by 100%.

Cellular Uptake of DOX

MCF-7 cells (HSA+) and HeLa cells (HSA-) were seeded in 6-well plates and incubated for 24 hours in humidified air at 37 °C and 5% CO_2. Cells were then treated with DOX-Lip or HSA-DOX-Lip (at a concentration of 200 μM DPPC) and were returned to the same previous incubation conditions for 1 hour, one plate of each cell line was exposed to LFUS (35-kHz) for 1 min using a sonicating bath. The cells were then harvested, pelleted and resuspended in PBS buffer for fluorescence analysis using flow cytometry measurements (Beckman Coulter FC500). The excitation wavelength used was 488 nm and DOX fluorescence was detected at 585 nm.

Statistical Analysis

Comparative statistical analysis was carried out to compare experimental groups' mean values. The two-tailed independent samples t-test with the equal variance assumption was carried out for (1) characterization tests, (2) MTT results and (3) the drug release data collected at all intensities. All results with $p < 0.05$ were considered statistically significant. All experimental values are reported as mean $\pm$ SD %, $n = 3$.

RESULTS AND DISCUSSION

Characterization and Stability of the Liposomes

The hydrodynamic radius of the prepared conjugated and non-conjugated stealth liposomes loaded with DOX as well as their polydispersity indices and size distribution, were measured using the DLS instrument. The obtained measurements are summarized in Table I. Statistical analysis of the hydrodynamic radius proved no significant differences between the size of the control liposomes and that of the conjugated ones ($p = 0.817$). Furthermore, the percent polydispersity index was lower than 20% for both types of liposomes. Figure 2 shows the size distribution graph of the DOX-Lip and HSA-DOX-Lip.

The average ratio of phospholipid concentration for HSA-DOX-lip to DOX-lip, measured using the Stewart assay, was found to be 0.917, demonstrating that both types of liposomes had a similar quantity of phospholipids ($p = 0.695$). In addition, the concentration of proteins present on the surface of the liposomes was estimated using the BCA assay and was calculated using the phospholipids concentrations. Higher ratios (1.5-fold increase) in protein content were found in all 3 batches of the HSA-DOX-lip (0.037 ± 0.004 μg/mL) compared to the

Table I. Size and polydispersity of DOX-liposomes and HSA-DOX-liposomes.

Liposomes	Radius (nm)	pd%
DOX-lip	85.1 ± 4.73	11.3 ± 0.59
HSA-DOX-lip	86.0 ± 2.50	11.6 ± 0.54

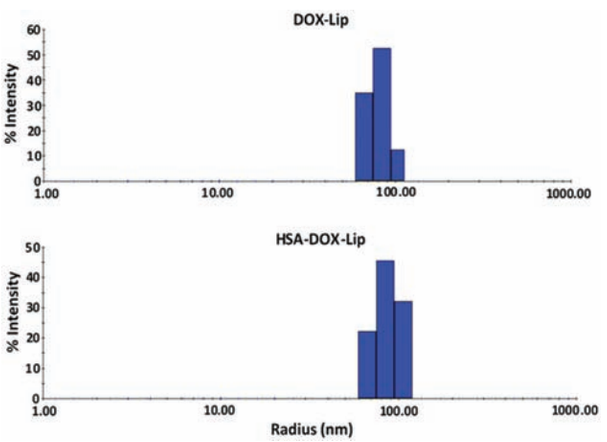

Figure 2. Size distribution graph for the DOX-Lip and HSA-DOX-Lip.

DOX-Lip (0.017 ± 0.001 μg/mL) indicating the successful conjugation of HSA molecules to the PEGylated (stealth) liposomes ($p = 2.71 \times 10^{-3}$). Both types of liposomes showed an encapsulation efficiency of 55%.

The stability of the prepared liposomes was investigated by monitoring the change in liposomes' sizes following their incubation in 10% fetal bovine serum (FBS) for 24 hours at 37 °C. No significant changes in the hydrodynamic radius of the DOX-lip (85.4 ± 1.6, $p = 0.942$) and their polydispersity ($11.6\% \pm 0.25$, $p = 0.963$) following the incubation period. HSA-DOX-lip were also stable, showing a hydrodynamic radius of (85.8 ± 2.7, $p = 0.873$) and a polydispersity percentage of (12.06 ± 0.18, $p = 0.625$) following the same incubation period.

HSA conjugation to the liposomes had no significant effect on the size and uniformity of these nanocarriers. Both liposomes were less than 200 nm in diameter and largely uniform in size, with a polydispersity percentage of less than 12%. We have previously used TEM images to show that protein molecules' conjugation to the surface of the liposomes caused no structural changes to the liposomes due to the small size of the targeting molecules compared to the stealth liposomes [20]. HSA conjugation also had no effect on the stability of the liposomes, with both types of liposomes maintaining their integrity following their incubation in FBS (10%) at 37 °C for 24 hours, showing no change in their size and thus showed no aggregation. A stable size of the liposomes is an indicator of the stability of liposomal suspensions [21, 22]. It was previously shown that the stability of the different nanocarriers in serum provides a good prediction of their stability during blood circulation [23, 24].

LFUS-Triggered Drug Release Kinetics

Sonicating the liposomes at low frequency to trigger DOX release from both DOX-Lip and HSA-DOX-Lip (3 batches each with three replicates per batch) was carried out using a 20-kHz probe at three increasing power densities (6.2 mW/cm^2, 9 mW/cm^2 and 10 mW/cm^2). The release was monitored by tracking changes in the fluorescence intensity of the released DOX. The normalized-averaged release profile for the DOX-Lip and HSA-DOX-lip are shown in Figure 3. A steep increase in the fluorescence intensity was recorded during the "on" phase of the pulsed sonication period. In contrast, no increase in DOX fluorescence was observed when LFUS was paused for 10 seconds during each pulse (the ultrasound "off" phase). Moreover, it can be seen from the averaged release profiles of the DOX-Lip and HSA-DOX-Lip that DOX release increased as the power density increased. A two-tailed *t*-test was performed on all types of tested liposomes for each power density.

A comparative study of DOX release from the DOX-lip and HSA-DOX-lip following the first three pulses of LFUS was conducted in terms of percentage fraction release,

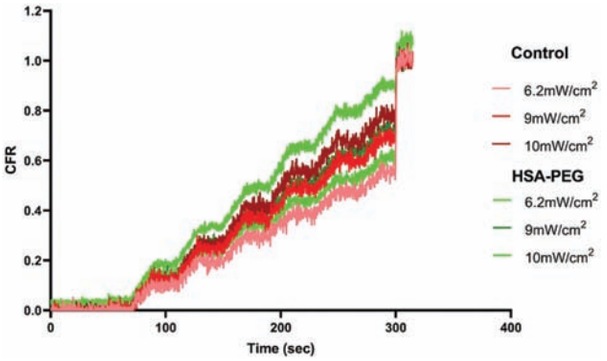

Figure 3. Normalized-averaged release profiles of 3 batches of DOX-Lip and HSA-DOX-Lip.

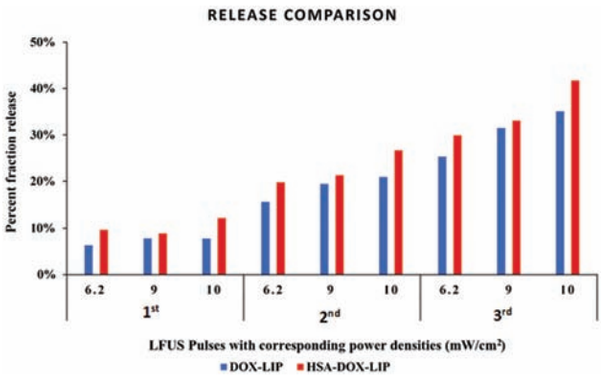

Figure 4. Percentage DOX release from DOX-Lip and HSA-DOX-Lip following the exposure to the first three pulses of LFUS at the different power densities 6.2, 9 and 10 mW/cm^2 expressed in terms of percentage fraction release.

as shown in Figure 4. In general, DOX release from both types of liposomes was clearly shown to increase in response to the increase in power density.

The statistical analysis of the results showed that the percentage of DOX released after the first pulse increased significantly ($p < 0.05$) as the power density increased for both DOX-lip and HSA-DOX-lip. A similar pattern was observed in the percentage DOX release following the second and third pulses ($p < 0.05$) for both types of liposomes. Calculated p-values are summarized in Table II. In addition, the statistical analysis showed that HSA-DOX-lip exhibited higher fraction release when compared to the DOX-lip at all three power densities investigated in our experiments ($p < 0.05$).

We have shown here that applying LFUS waves on liposomes loaded with DOX resulted in triggering DOX release from the liposomes in a controlled manner. DOX release was triggered during the "on" phase of the pulse only, which lasted for 20 seconds, and stopped completely during the "off" phase, which lasted for 10 seconds. Furthermore, DOX release rate was proportional to the power density used, with the highest rate reported at the highest power density used (i.e., 10 mW/cm^2). As the

Table II. Statistical comparison of fraction release values at different power densities used (mW/cm^2) during the first three pulses of LFUS.

DOX-lip			
Power density	1st pulse	2nd pulse	3rd pulse
6.2 versus 9	0.0269	1.129×10^{-5}	2.778×10^{-18}
9 versus 10	6.323×10^{-7}	4.752×10^{-23}	4.959×10^{-39}
6.2 versus 10	1.796×10^{-11}	1.441×10^{-34}	1.316×10^{-60}
HSA-DOX-lip			
6.2 versus 9	0.135	0.00450	2.116×10^{-8}
9 versus 10	2.090×10^{-7}	2.383×10^{-15}	$8.881\ 10^{-29}$
6.2 versus 10	2.392×10^{-5}	1.283×10^{-24}	6.984×10^{-45}

waves produced by the LFUS propagate through the liquid surrounding the cells, the produced cavitation causes physical effects on the phospholipid bilayer surrounding the cells, resulting in forming transient pores which are able to reseal once ultrasound is turned off [25]. This is known as the sonoporation process and has been used to deliver genes and large molecules to the cells. Sonoporation occurs due to both stable and transient cavitation. Oscillation of the air bubbles formed during the stable cavitation process causes oscillatory stresses by pushing and pulling the nearby cellular membranes. In addition, other mechanical stresses are generated by the shear stresses and the microjets produced due to inertial cavitation. All or some of these mechanical stresses could be the driving force behind the sonoporation phenomenon [26, 27]. In addition to the mechanical effects, LFUS also produces a thermal effect but to a lower level compared to high-frequency ultrasound (HFUS).

Liposomes are also made from a phospholipid bilayer. Therefore, applying LFUS waves to the liposomal solution will also affect the permeability of the liposomes by forming transient pores on their membranes. As shown here, applying pulsed LFUS resulted in triggering DOX release from both DOX-lip and HSA-DOX-lip, and the release rate increased with the increasing power density. This indicates that more pores are formed as the power density increases. DOX release was triggered during the "on" phase of the LFUS. However, during the "off" phase of the pulsed LFUS, the pores can reseal, resulting in a "freeze" or "lull" in DOX release from the liposomes. We have previously shown that applying pulsed LFUS reduced the size of the liposomes while increasing their polydispersity percentage regardless of the power density used [28]. This could be due to the phospholipid bilayer's loss during the repeated pore-forming and resealing process. As mentioned earlier, an increase in the temperature can be caused by the cavitation events produced by the ultrasound waves. A temperature rise above the transition temperature of the phospholipids (the temperature required for the transition from the gel phase to the liquid phase) will also trigger DOX release from the liposomes. As seen in Figure 4, both types of liposomes showed strong DOX release following the first three pulses of LFUS. There was no temperature rise with the lower power densities. However, when the highest power density was used, we observed a 6-degree temperature rise (from 25 °C to 31 °C), which is still below the transition temperature of the DPPC (i.e., 41.3 °C). Therefore, we measured DOX release following increasing the temperature of the liposomes to 31 °C with no sonication and found that DOX-lip and HSA-DOX-lip released only 7% and 2.1% of their loaded DOX upon heating compared to 36% and 42%, respectively when sonicated. This indicates that despite a possible thermal effect, the cavitation process is the primary mechanism behind the reported DOX release.

We have also shown that the targeted liposomes (HSA-DOX-lip) were more sonosensitive compared to the non-targeted liposomes (DOX-lip). A possible explanation of this phenomenon is that the application of LFUS may force the interaction between HSA molecules and the phospholipid bilayer of the liposomes. A previous study by Thakur et al. [29] investigated the interaction between HSA and the phospholipids forming the liposomes using the circular dichroism analysis that monitors the conformational changes in proteins and anisotropy measurement. The study showed that DPPC phospholipids have a high affinity toward HSA molecules and form hydrophobic interactions between liposomes and HSA molecules, allowing HSA molecules to penetrate through the bilayer and alter/change the packing order of the formed liposome. Also, we have previously shown that liposomes conjugation to a small peptide (RGD) and a large hydrophilic polymer (hyaluronic acid) did not affect the sonosensitivity of the liposomes [20, 30], which indicates that the structure of the conjugated molecule may play a role in affecting the sensitivity of the conjugated liposomes to ultrasound waves.

In Vitro Cellular Uptake and Cytotoxicity Analysis

Cellular uptake of DOX encapsulated inside DOX-Lip and HSA-DOX-Lip was measured "*in vitro*" using flow cytometry analysis. As seen in Figure 5(A), when loaded liposomes were incubated with MCF-7 (HAS + cell line), a 168% increase in cellular uptake of DOX was recorded in the cells incubated with targeted liposomes (HSA-DOX-Lip), showing a mean fluorescent intensity (MFI) value of 68671.34 ± 2783.9 compared to those incubated with non-targeted liposomes (DOX-Lip) which showed MFI value of 25607 ± 992.2 ($p = 3.3 \times 10^{-5}$). This showed that HSA conjugation to the liposomes enhanced cellular uptake of the encapsulated DOX. Furthermore, sonicating the cells incubated with HSA-DOX-Lip significantly enhanced DOX uptake showing MFI value of 92008.7 ± 5229.5 ($p = 0.005$) and thus, exhibiting a 259.3% increase in DOX uptake compared to the non-conjugated liposomes ($p = 6.06 \times 10^{-5}$).

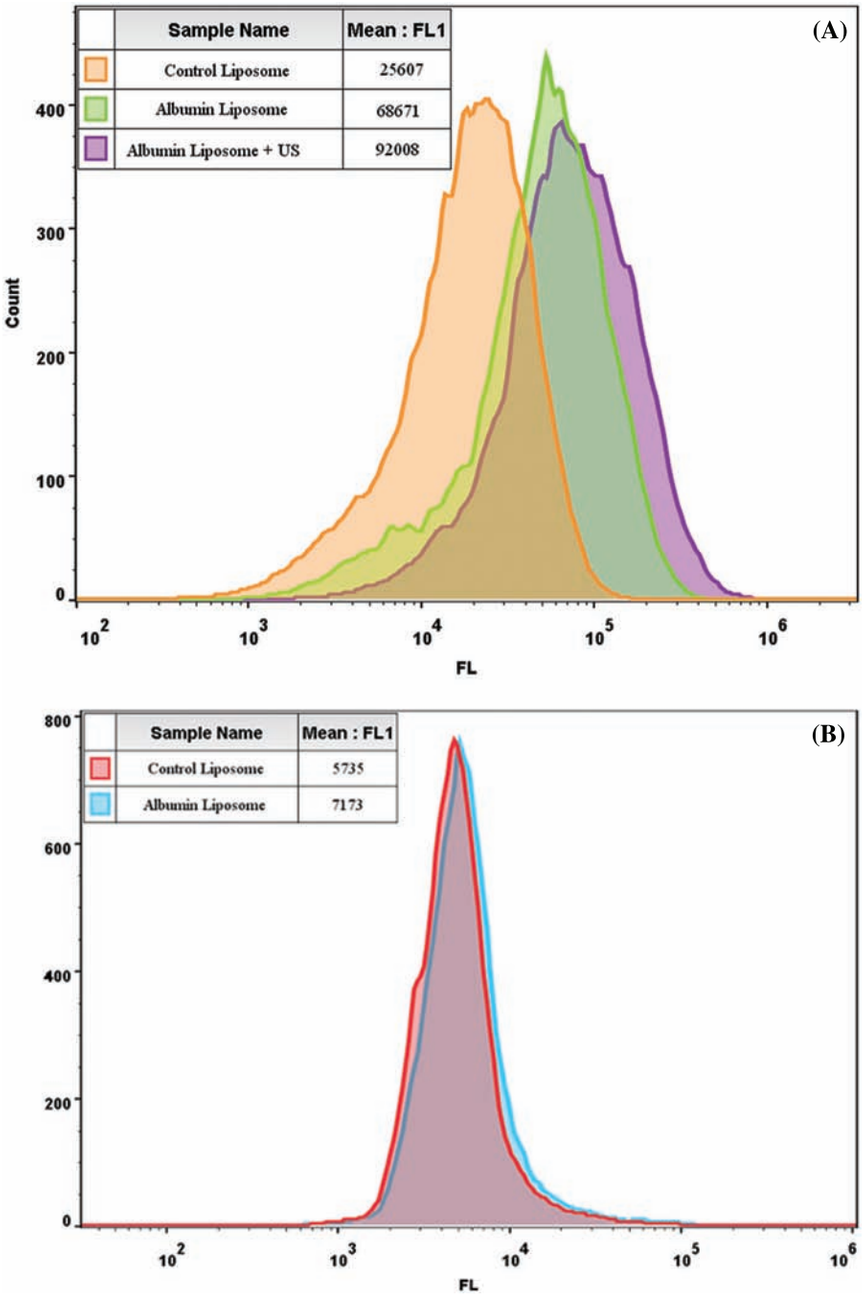

Figure 5. **(A) Shows DOX uptake by MCF-7 cells (HSA+) following their incubation with DOX-Lip or HSA-DOX-Lip for 1 hour, HSA conjugation to the liposomes resulted in a significant increase in cellular uptake of DOX which was further enhanced when exposing the cells to LFUS for 1 minute. On the contrary, (B) shows DOX uptake by HeLa cells (HSA-), where no significant differences in cellular uptake of DOX was recorded following their incubation with both types of liposomes. Data are representative of three independent experiments (mean ± SD %, $n = 3$).**

To prove that the observed improvement in DOX uptake by the cells was due to the binding of the targeted liposomes to albumin receptors present in the cells, the same experiment was repeated using HSA- cell line (HeLa cells). As seen in Figure 5(B), no significant difference was observed in DOX MFI values between DOX-Lip (5734.4 ± 329.5) and HSA-DOX-Lip ($7173.3 \pm$) ($p =$ 0.091). This indicates that DOX uptake by HeLa cells was not affected by the presence of HSA as a targeting ligand on the liposomes. The results show that HSA conjugation to the liposomes will enhance cellular uptake of the encapsulated drugs by cancer cells expressing HSA receptors on their surfaces. This will facilitate the binding of these liposomes to the cells and the subsequent enhancement of

cellular uptake of the loaded drugs. Combining targeted liposomes with LFUS will further enhance cellular uptake of drugs by triggering drug release from the liposomes in a controlled manner. This will effectively target specific cancer cells and enhance drug efficiency while reducing their unwanted systemic toxicity.

To assess the cytotoxic activity of the prepared liposomes in the presence and absence of LFUS as a triggering mechanism, the MTT assay was performed using both MCF-7 human cancer cells (HSA+) and HeLa cells (HSA−) cells. The results are depicted in Figure 6. Unloaded liposomes were used as vehicle control to confirm the biocompatibility of the investigated liposomes and showed no effects on the viability of both cells lines used here, proving that any induced cytotoxic effects are due to the DOX action and not the nanocarriers. Furthermore, sonicating the cells with LFUS with no drug/liposomes added did not affect cell viability indicating that the used LFUS (35 kHz) is a safe triggering mechanism and had no toxic effects on the cells.

Figure 6(A) shows the cell viabilities of MCF-7 in response to treatments with free DOX, DOX-Lip and HSA-DOX-Lip, in the presence and absence of LFUS as a triggering mechanism. When no ultrasound was applied, the percent of viable cells treated with free DOX, DOX-Lip and HSA-DOX-Lip were found to be 30.8 ± 3.37, 68.8 ± 0.96 and 46.1 ± 4.2, respectively. Both liposomal formulations imposed considerable noxious effects on the cells. Yet, the cytotoxic action of HSA-DOX-Lip was superior to the DOX-Lip ($p = 1.6 \times 10^{-2}$). Sonication with

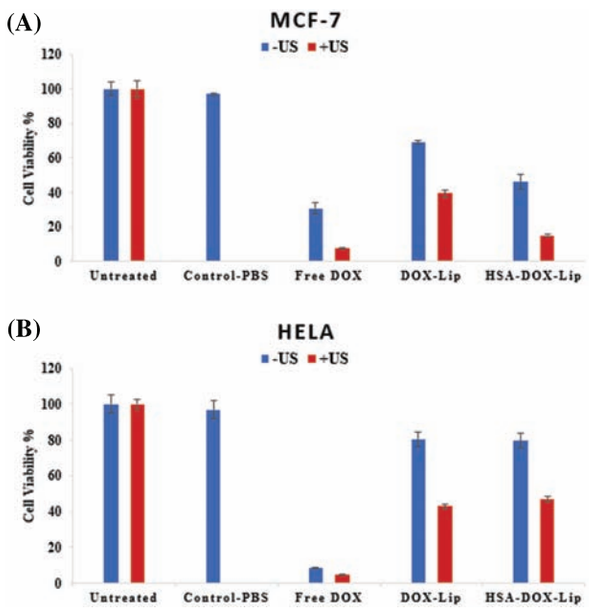

Figure 6. MTT results for MCF-7 cells (A) and HeLa cells (B) treated with free DOX, DOX-liposomes and HSA-DOX-liposomes without exposure to LFUS (-US) and with sonication at 35 kHz for 1 min (+US). Data are representative of three independent experiments (mean ± SD %, $n = 3$).

LFUS lowered the percentage cell viability significantly compared to the non-sonicated cells when treated with free DOX (7.96 ± 0.12; $p = 1.3 \times 10^{-2}$), DOX-Lip (39.5 ± 0.50; $p = 1.9 \times 10^{-3}$) and HSA-DOX-Lip (15.1 ± 0.60; $p = 6.3 \times 10^{-4}$).

To investigate whether HSA-DOX-lip can only enhance drug delivery to HSA+ cells, the MTT assay was repeated using HeLa (HSA-) cells. As shown in Figure 6(B), no significant difference in cell viability between the cells treated with DOX-Lip and HSA-DOX-Lip was recorded, with percent cell viability of 80.5 ± 0.449 and 79.6 ± 0.262, respectively ($p = 2.37 \times 10^{-1}$). This indicates that HSA conjugation to the surface of the liposomes had no effect on the liposomal cytotoxicity to HeLa cells. Sonication with LFUS lowered the viabilities of cells treated with both DOX-lip and HSA-DOX-lip, i.e., 43.0 ± 4.30 and $47.3 \pm 0.62\%$, respectively.

Incubation of free DOX with both MCF-7 and HeLa cells showed the highest toxicity compared to both types of DOX-loaded liposomes. The toxicity of the free DOX was enhanced upon sonication with LFUS (35 kHz). This could be caused by the sonoporation and enhanced permeability caused by the LFUS, which results in higher DOX uptake by the cells. In addition, ultrasound applied alone had no toxic effect on the cells (Fig. 6). This is in agreement with a recent study by Eikrem et al. [31], which reported that applying ultrasound improved the delivery of DOX to mouse kidney tissues while causing no longstanding damage. The high expression level of HSA receptors on the surface of MCF-7 cells resulted in the binding of HSA-DOX-lip to those receptors and the subsequent increase in DOX uptake and enhanced cytotoxicity. On the other hand, HSA conjugation to the liposomes had no effect on their cytotoxicity when incubated with HeLa cells due to the low expression levels of HSA receptors. Our findings support results previously reported by our group [32]. Flow cytometry analysis showed that the cellular uptake of albumin-bound liposomes encapsulating the model drug calcein was significantly higher in MCF-7 cells compared to HeLa cells, confirming that surface modification of the liposomes with HSA ligands enhanced their binding affinity and active uptake via mediated endocytosis. Compared to the control liposomes, uptake of the albumin-bound liposomes by the positive cell line increased by 90%. The increased affinity of MCF-7 cells towards HSA-decorated drug carriers was also scrutinized by Jiang and colleagues [33]. The effect of conjugating nanoparticles with different albumin concentrations on the cellular uptake of several cell lines was examined. The uptake of the nanoparticles by the MCF-7 cells increased as their surface albumin content increased.

Applying LFUS increased the cytotoxic effect of all the liposomal formulations in both cell lines. This is due to the enhanced permeability of both the cellular and liposomal membranes resulting in higher DOX uptake. The

synergistic action of insonation and HSA-DOX-lip formulation showed a drop in cell viabilities % from 46.1 ± 4.2 to 15.1 ± 0.60 ($p = 1.5 \times 10^{-2}$), signifying a promising platform for the treatment of cancer cells overexpressing HSA receptors. To develop an optimized system, it is necessary to undertake further analysis by manipulating incubation time, liposomal formulations, and LFUS-associated parameters such as frequency, power density, and exposure time. This work was studied using *in vitro* analysis to understand the behavior of the DOX-loaded liposomes while mimicking the body temperature and pH to prove the concept of controlling DOX release from targeted and non-targeted liposomes using LFUS. However, the blood circulation effect should be the subject of future work, including *in vivo* and clinical studies, to further understand and develop this promising therapeutic platform.

CONCLUSIONS

The ability of targeted liposomes loaded with antineoplastic drugs, such as Doxorubicin, to extravasate through the leaky vasculature surrounding the tumors (i.e., EPR effect) and bind to the targeted tumor cells before their uptake by the cells (endocytosis) is a promising drug delivery modality. However, it is essential to ensure that those nanocarriers are able to fully release their load following their accumulation inside the tumor tissues. Therefore, developing an effective drug release triggering mechanism is necessary to unlock the full potential of liposomes as smart drug delivery vehicles. In this study, we conducted several *in vitro* experiments to investigate the ability of LFUS to trigger DOX release from targeted liposomes prepared from stealth liposomes functionalized with HSA as a targeting ligand. We aimed to understand how LFUS triggers DOX release from the liposomes, at different power densities, and whether the presence of a targeting ligand on the surface of those liposomes affects the LFUS-triggered drug release from the liposomes. We also examined the effect of combining LFUS with targeted liposomes on the cytotoxicity of DOX using both HSA+ and HSA- cancer cell lines.

The synthesis, characterization and *in vitro* LFUS-triggered DOX release from HSA-DOX-Lip and DOX-loaded liposomes and their cytotoxicity with and without ultrasound application were thoroughly studied. Size measurements of the control liposomes loaded with DOX and the HSA-conjugated liposomes revealed that functionalization had no significant effects on the size and stability of the liposomes, and both types fall within the acceptable size range, and thus can benefit from the EPR effect. LFUS triggered DOX release from the liposomes, and the release rate increased with the increase in the power density. HSA-DOX-liposomes were found to be more sonosensitive compared to DOX-lip. The *in vitro* assessment of using different cell lines in the presence and absence of LFUS exposure suggested that coupling LFUS with targeted liposomes elicits synergistic effects and enhanced drug uptake by the targeted cells. Our findings represent a starting point for future optimization efforts to translate this technology into clinics.

Ethical Compliance

Research experiments conducted in this article with animals or humans were approved by the Ethical Committee and responsible authorities of our research organization(s) following all guidelines, regulations, legal, and ethical standards as required for humans or animals.

Conflicts of Interest

The authors declare no conflict of interest.

Acknowledgments: The authors would like to acknowledge the financial support of the American University of Sharjah Faculty Research Grants, the Al-Jalila Foundation (AJF 2015555), the Al Qasimi Foundation, the Patient's Friends Committee-Sharjah, the Biosciences and Bioengineering Research Institute (BBRI18-CEN-11), GCC Co-Fund Program (IRF17-003) the Takamul program (POC-00028-18), the Technology Innovation Pioneer (TIP) Healthcare Awards, Sheikh Hamdan Award for Medical Sciences (MRG-57-2019-2020), Friends of Cancer Patients (FoCP) and the Dana Gas Endowed Chair for Chemical Engineering. We also would like to acknowledge student funding from the Material Science and Engineering Ph.D. program at AUS.

REFERENCES

1. Sudhakar, A., **2009**. History of cancer, ancient and modern treatment methods. *Journal of Cancer Science & Therapy*, *1*(2), p.1.
2. Liu, D., Yang, F., Xiong, F. and Gu, N., **2016**. The smart drug delivery system and its clinical potential. *Theranostics*, *6*(9), p.1306.
3. Motevalli, S.M., Eltahan, A.S., Liu, L., Magrini, A., Rosato, N., Guo, W., Bottini, M. and Liang, X.J., **2019**. Co-encapsulation of curcumin and doxorubicin in albumin nanoparticles blocks the adaptive treatment tolerance of cancer cells. *Biophysics Reports*, *5*(1), pp.19–30.
4. Yang, W.H., Ding, M.J., Cui, G.Z., Yang, M. and Dai, D.L., **2018**. Heterogeneous nuclear ribonucleoprotein M promotes the progression of breast cancer by regulating the axin/β-catenin signaling pathway. *Biomedicine & Pharmacotherapy*, *105*, pp.848–855.
5. Sun, H., Liu, T., Zhu, D., Dong, X., Liu, F., Liang, X., Chen, C., Shao, B., Wang, M. and Wang, Y., **2017**. HnRNPM and CD44s expression affects tumor aggressiveness and predicts poor prognosis in breast cancer with axillary lymph node metastases. *Genes, Chromosomes and Cancer*, *56*(8), pp.598–607.
6. Dreher, M.R., Liu, W., Michelich, C.R., Dewhirst, M.W., Yuan, F. and Chilkoti, A., **2006**. Tumor vascular permeability, accumulation, and penetration of macromolecular drug carriers. *Journal of the National Cancer Institute*, *98*(5), pp.335–344.
7. Milla, P., Dosio, F. and Cattel, L., **2012**. PEGylation of proteins and liposomes: A powerful and flexible strategy to improve the drug delivery. *Current Drug Metabolism*, *13*(1), pp.105–119.
8. Kim, E.M. and Jeong, H.J., **2021**. Liposomes: Biomedical applications. *Chonnam Medical Journal*, *57*(1), p.27.

9. Schroeder, A., Kost, J. and Barenholz, Y., **2009**. Ultrasound, liposomes, and drug delivery: Principles for using ultrasound to control the release of drugs from liposomes. *Chemistry and Physics of Lipids*, *162*(1–2), pp.1–16.

10. Martins, A.M., Ahmed, S.E., Vitor, R.F. and Husseini, G., **2016**. Ultrasonic drug delivery using micelles and liposomes.

11. De Matos, M.B., Deckers, R., Van Elburg, B., Lajoinie, G., de Miranda, B.S., Versluis, M., Schiffelers, R. and Kok, R.J., **2019**. Ultrasound-sensitive liposomes for triggered macromolecular drug delivery: Formulation and *in vitro* characterization. *Frontiers in Pharmacology*, *10*, p.1463.

12. Schroeder, A., Honen, R., Turjeman, K., Gabizon, A., Kost, J. and Barenholz, Y., **2009**. Ultrasound triggered release of cisplatin from liposomes in murine tumors. *Journal of Controlled Release*, *137*(1), pp.63–68.

13. Husseini, G.A., De La Rosa, M.A.D., Richardson, E.S., Christensen, D.A. and Pitt, W.G., **2005**. The role of cavitation in acoustically activated drug delivery. *Journal of Controlled Release*, *107*(2), pp.253–261.

14. Husseini, G.A. and Pitt, W.G., **2009**. Ultrasonic-activated micellar drug delivery for cancer treatment. *Journal of Pharmaceutical Sciences*, *98*(3), pp.795–811.

15. Apfel, R.E. and Holland, C.K., **1991**. Gauging the likelihood and degree of cavitational activity from diagnostic ultrasound. *Ultrasound Med. Biol.*, *17*, pp.179–185.

16. Zhang, H., **2017**. Thin-film hydration followed by extrusion method for liposome preparation. in *Liposomes*. New York, NY, Humana Press, pp.17–22.

17. Fritze, A., Hens, F., Kimpfler, A., Schubert, R. and Peschka-Süss, R., **2006**. Remote loading of doxorubicin into liposomes driven by a transmembrane phosphate gradient. *Biochimica et Biophysica Acta (BBA)-Biomembranes*, *1758*(10), pp.1633–1640.

18. Tacar, O., Sriamornsak, P. and Dass, C.R., **2013**. Doxorubicin: An update on anticancer molecular action, toxicity and novel drug delivery systems. *Journal of Pharmacy and Pharmacology*, *65*(2), pp.157–170.

19. Riss, T.L., Moravec, R.A., Niles, A.L., Duellman, S., Benink, H.A., Worzella, T.J. and Minor, L., **2016**. Cell viability assays. *Assay Guidance Manual [Internet]*.

20. Awad, N.S., Paul, V., Mahmoud, M.S., Al Sawaftah, N.M., Kawak, P.S., Al Sayah, M.H. and Husseini, G.A., **2019**. Effect of pegylation and targeting moieties on the ultrasound-mediated drug release from liposomes. *ACS Biomaterials Science & Engineering*, *6*(1), pp.48–57.

21. Muppidi, K., Pumerantz, A.S., Wang, J. and Betageri, G., **2012**. Development and stability studies of novel liposomal vancomycin formulations. *International Scholarly Research Notices*, *2012*.

22. Wehbe, M., Malhotra, A., Anantha, M., Roosendaal, J., Leung, A.W., Plackett, D., Edwards, K., Gilabert-Oriol, R. and Bally, M.B., **2017**. A simple passive equilibration method for loading carboplatin into pre-formed liposomes incubated with ethanol as a temperature dependent permeability enhancer. *Journal of Controlled Release*, *252*, pp.50–61.

23. Lin, W., Ma, G., Yuan, Z., Qian, H., Xu, L., Sidransky, E. and Chen, S., **2018**. Development of zwitterionic polypeptide nanoformulation with high doxorubicin loading content for targeted drug delivery. *Langmuir*, *35*(5), pp.1273–1283.

24. Bauer, K.N., Simon, J., Mailänder, V., Landfester, K. and Wurm, F.R., **2020**. Polyphosphoester surfactants as general stealth coatings for polymeric nanocarriers. *Acta Biomaterialia*, *116*, pp.318–328.

25. Wang, M., Zhang, Y., Cai, C., Tu, J., Guo, X. and Zhang, D., **2018**. Sonoporation-induced cell membrane permeabilization and cytoskeleton disassembly at varied acoustic and microbubble-cell parameters. *Scientific Reports*, *8*(1), pp.1–12.

26. Awad, N.S., Paul, V., AlSawaftah, N.M., Ter Haar, G., Allen, T.M., Pitt, W.G. and Husseini, G.A., **2021**. Ultrasound-responsive nanocarriers in cancer treatment: A review. *ACS Pharmacology & Translational Science*, *4*(2), pp.589–612.

27. Bouakaz, A., Zeghimi, A. and Doinikov, A.A., **2016**. Sonoporation: Concept and mechanisms. *Therapeutic Ultrasound*, pp.175–189.

28. AlSawaftah, N.M., Awad, N.S., Paul, V., Kawak, P.S., Al-Sayah, M.H. and Husseini, G.A., **2021**. Transferrin-modified liposomes triggered with ultrasound to treat HeLa cells. *Scientific Reports*, *11*(1), pp.1–15.

29. Thakur, R., Das, A. and Chakraborty, A., **2014**. Interaction of human serum albumin with liposomes of saturated and unsaturated lipids with different phase transition temperatures: A spectroscopic investigation by membrane probe PRODAN. *RSC Advances*, *4*(28), pp.14335–14347.

30. Ben Daya, S.M., Paul, V., Awad, N.S., Al Sawaftah, N.M., Al Sayah, M.H. and Husseini, G.A., **2021**. Targeting breast cancer using hyaluronic acid-conjugated liposomes triggered with ultrasound. *Journal of Biomedical Nanotechnology*, *17*(1), pp.90–99.

31. Eikrem, O., Kotopoulis, S., Popa, M., Mayoral Safont, M., Fossan, K.O., Leh, S., Landolt, L., Babickova, J., Gudbrandsen, O.A., Gilja, O.H. and Riedel, B., **2021**. Ultrasound and microbubbles enhance uptake of doxorubicin in murine kidneys. *Pharmaceutics*, *13*(12), p.2038.

32. Awad, N.S., Paul, V., Al-Sayah, M.H. and Husseini, G.A., **2019**. Ultrasonically controlled albumin-conjugated liposomes for breast cancer therapy. *Artificial Cells, Nanomedicine, and Biotechnology*, *47*(1), pp.705–714.

33. Jiang, Y., Wong, S., Chen, F., Chang, T., Lu, H. and Stenzel, M.H., **2017**. Influencing selectivity to cancer cells with mixed nanoparticles prepared from albumin–polymer conjugates and block copolymers. *Bioconjugate Chemistry*, *28*(4), pp.979–985.